Polymer Journal, Vol. 12, No. 5, pp 305—317 (1980)

Aggregated States and Solidifying Process of α-Helical Molecular Chains of Poly(γ-methyl glutamate)

Ken'ichi ITO,*[1] Tisato KAJIYAMA,*[1] and Motowo TAKAYANAGI*[1]

*[1] *Department of Applied Chemistry, Faculty of Engineering, Kyushu University, 36 Hakozaki, Fukuoka 812, Japan.*

(Received October 16, 1979)

ABSTRACT: The aggregated states of molecular chains of poly (γ-methyl glutamate) in various solvents were studied by means of X-ray diffraction and light scattering techniques. In this study, α-helical chains in a *m*-cresol system were homogeneously dispersed and formed a stable cholesteric liquid crystal over a wide range of temperature, from the solvent melting point to 400 K at a relatively low concentration (30 wt%), while the highly concentrated solution existed in the form of a paracrystalline phase with a two-dimensional hexagonal lattice including solvent molecules. In the pyridine system, the solution was gelatinized and α-helical chains aggregated to form a gel network. Both differential scanning calorimetry and optical microscopic observation revealed that the gel and cholesteric phases were mutually reversible depending on the temperature in the case of the pyridine solution.

KEY WORDS Poly(γ-methyl glutamate) / Aggregated State / Cholesteric Liquid Crystal / Small-Angle Light Scattering / Differential Scanning Calorimetry / Polarizing Micrograph /

The authors have already reported on the aggregated state of α-helical molecular chains in well annealed films of poly(γ-methyl D-glutamate) cast from various solutions.[1] A planar orientation, in which the *c* crystal axis is oriented parallel to a reference plane,[2] was observed when the films were cast from cholesteric solutions in chloroform, 1,2-dichloroethane, *m*-cresol, and so on. On the other hand, a $(10\bar{1}0)$ uniplanar orientation of crystallites, in which the α-helices are packed in hexagonal array, was observed in well annealed films cast from solutions in pyridine, dioxane, trichloroethylene, and so on, whose concentrated solutions formed a gel phase at room temperature. In the case of a uniplanar orientation, a crystal plane is oriented parallel to the reference plane, which also satisfies the plane definition.[2] The former solvents which induced the formation of a planar orientation were termed by the authors as "Group 1" solvents and the latter which induced the formation of a $(10\bar{1}0)$ uniplanar orientation were termed "Group 2" solvents.[1] The classification of these solvents is listed in Table I. It is apparent that aggregated states in a concentrated solution affect aggregated states in the solid states.

Robinson[3] studied the packed states of poly(γ-benzyl L-glutamate) (PBLG) molecules in dioxane, using the X-ray diffraction technique and concluded that PBLG molecules were uniformly dispersed in hexagonal array in a cholesteric liquid crystal phase. He suggested that the $(11\bar{2}0)$ plane of hexagonal aggregates is perpendicular to the twist axis of the cholesteric liquid crystal which is perpendicular to the film surface.

Luzzati[4] suggested that the aggregated states in concentrated solutions of PBLG in *m*-cresol, pyridine, and dimethylformamide varied, depending on both solvent and polymer concentration. He found three types of phase with increase of polymer concentration on the basis of the results of small-angle X-ray scattering: (1) the paracrystalline phase transformed from the cholesteric phase in PBLG-*m*-cresol system, (2) the complex phase transformed from the cholesteric phase in PBLG–pyridine system, and (3) the complex phase in PBLG–dimethylformamide system existing from the beginning. He also reported the structure of the complex phase modified later by Parry.[5,6] The complex phase is characterized by the stacking of phenyl rings located at the end portion of the side chains of PBLG.

Table I. Classification of solvents based on the type of the orientation for PMG film

	Solvents	Orientations
Group 1	Chloroform 1,2-Dichloroethane 1,1,2-Trichloroethane 1,2,3-Trichloropropane *cis*-Dichloroethylene *trans*-Dichloroethylene *m*-Cresol	Planar orientation
Group 2	Trichloroethylene Chlorobenzene *N,N*-Dimethylformamide Pyridine Dioxane	$(10\bar{1}0)$ Uniplanar orientation

Samulski[7] suggested that helicoidal structure exists in plastisized PBLG film. Tachibana[8] reported the existence of the cholesteric structure in poly(γ-methyl glutamate) (PMG) film based on circular dichroic studies; that is, the film consisting of D-isomer reflected selectively the left circularly polarized light, while that of L-isomer exhibited the opposite. Thus, from the manner of apparent absorbance for circularly polarized light, the existence, and the sense of the twist of macrohelix could be determined.

In this paper, we will discuss the aggregated state of the α-helical chains of PMG in various solvents and the influence of a given solvent upon the aggregated state in the solid state cast from the solution by using X-ray diffractometry, differential scanning calorimetry, and optical techniques.

EXPERIMENTAL

X-Ray Diffraction

Poly(γ-methyl D-glutamate) (PMDG, AJICOAT A-200, $M_v=140000$) was dissolved in *m*-cresol (Group 1), pyridine, and dioxane (Group 2). In the case of pyridine and dioxane, PMDG solutions were prepared by heating above 335 K and cooling down to room temperature. Solvents containing halogen atoms, such as chloroform and 1,2-dichloroethane, could not be used for X-ray diffraction measurement since they absorb X-ray beams, and diffractions responsible for the solution structure are not apparent. Solutions varying in concentration were poured into a sample cell containing a poly(tetrafluoroethylene) (PTFE) spacer and square windows of poly(ethylene terephthalate) (PET) films. The wide-angle X-ray photographs of these solutions were taken at 298 and 335 K with a rotating anode unit (Rota Unit RU-3, Rigaku Denki Co.). The Ni-filtered X-ray (Cu–K_α) beam was irradiated normal to the PET window.

Small-Angle Light Scattering

PMDG solutions in *m*-cresol and pyridine were set between two glass plates for small-angle light scattering (SALS) measurements. The light source was a He–Ne gas laser (wavelength 0.6328 μm). Polarizing optical microscopic (POM) observations were carried out for the same samples.

Differential Scanning Calorimetry

PMDG solutions in chloroform, 1,2-dichloroethane, 1,1,2-trichloroethane, *m*-cresol (Group 1), pyridine, and dioxane (Group 2) were sealed in aluminium pans in order to avoid solvent evaporation. Differential scanning calorimetry (DSC) measurements of these solutions were performed in a temperature range from 200 to 400 K (UNIX, Rigaku Denki Co.). In the case of 1,2-dichloroethane, poly(γ-methyl L-glutamate) (PMLG, AJICOAT A-2000, $M_v=60000$) was used. Heating and cooling rates were 2.5 K min^{-1}.

Circular Dichroic Measurement

Solid films of PMDG and PMLG cast from various solvents were used for circular dichroic (CD) measurements. The apparatus was a Jasco ORD/UV-5 or Jasco J-40AS (Xe-light source, 250—800 nm).

Electron Microscopic Observation

Dilute solutions in various solvents were dropped on copper meshes coated with carbon. After being dried, the samples were shadowed by Pt–Pd and offered to electron microscopic (EM) observation (H-500, Hitachi, Ltd.).

RESULTS AND DISCUSSION

m-Cresol Solution (Group 1)

Figure 1 shows the polarizing optical micrograph for a 30.6 wt% PMDG solution in *m*-cresol at 298 K, representing the retardation lines and irridescent

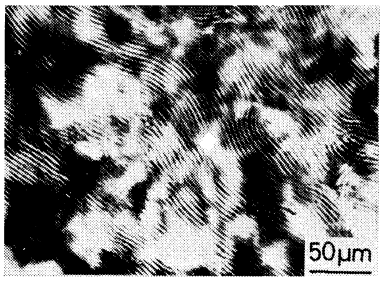

Figure 1. Polarizing optical micrograph for a 30.6 wt% PMDG solution in *m*-cresol at 298 K under crossed nicols.

colors characteristic of the cholesteric liquid crystal. Other solvent systems belonging to "Group 1" exhibited the same optical properties as the *m*-cresol system. The concentrations at the A-point of the PMDG solutions were 9, 9, 10, and 12 wt% for *m*-cresol, chloroform, 1,2-dichloroethane, and 1,1,2-trichloroethane systems, respectively.

Figure 2 shows the X-ray diffraction diagrams and their schematic patterns of *m*-cresol solutions of PMDG at 298 K. Below polymer concentration of 40 wt%, only one X-ray diffraction ring could be observed. Relatively sharp arcs at the outermost location are attributed to PET, used for the cell windows. Because the Bragg angle and sharpness of the diffraction ring increase with increasing polymer concentration, it seems reasonable to attribute the spacing of this diffraction to the distance between the neighboring α-helical chains. Though, in a lower concentration range of the *m*-cresol solution, PMDG molecules are aggregated in a fairly orderly fashion, the helicoidal structure in the cholesteric liquid crystal does not have a long range order. Thus, higher-order diffractions cannot be observed. In the case of polymer concentrations above 41 wt%, a drastic change in the diffraction diagram could be observed; that is, at least four rings appeared above 45 wt% as shown in Figure 2(c). This drastic change in the X-ray diffraction pattern may indicate some kind of change in the aggregated state. The ratios of the reciprocals of these four spacings were $1:\sqrt{3}:2:\sqrt{7}$. These ratios are the same as those of equatorial reflections from a hexagonal lattice and did not vary with polymer concentration.

Figure 3 shows the concentration dependence of the maximum spacing evaluated from the innermost diffraction ring as shown in Figure 2. The filled circles correspond to the data at 298 K, and open

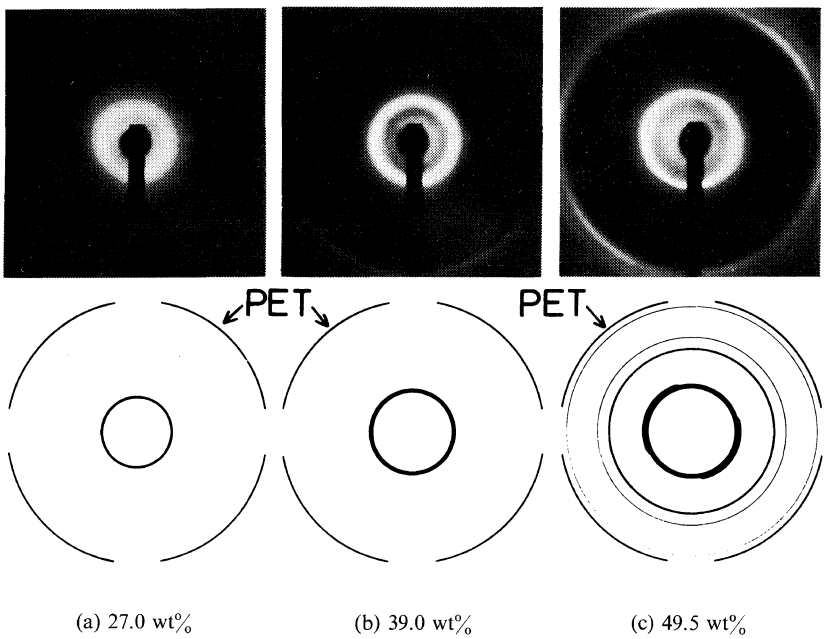

(a) 27.0 wt% (b) 39.0 wt% (c) 49.5 wt%

Figure 2. X-ray diffraction photographs and their schematic illustrations of PMDG solutions in *m*-cresol at various concentration: (a) 27.0 wt%, (b) 39.0 wt%, and (c) 49.5 wt% at 298 K.

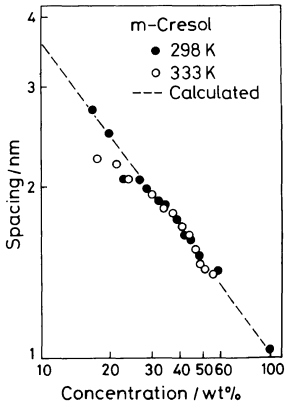

Figure 3. Concentration dependence of the spacing evaluated from the most inner X-ray diffraction ring for a PMDG solution in *m*-cresol at 298 K (filled circle) and 333 K (open circle). The broken line is a calculated one.[3]

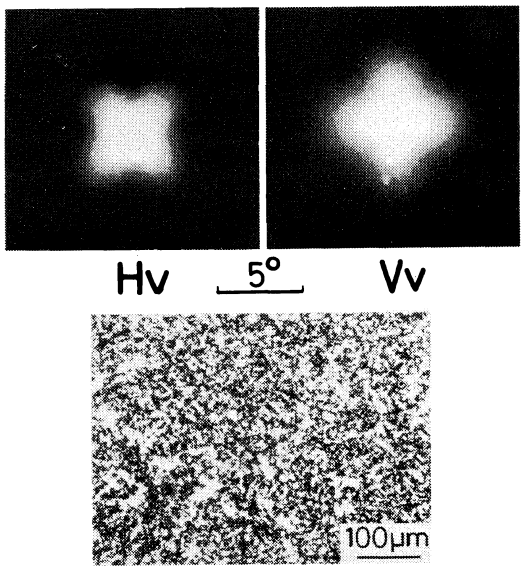

Figure 4. Small-angle light scattering (SALS) patterns and polarizing micrograph for a 49.7 wt% PMDG solution in *m*-cresol at 290 K.

circles, at 333 K. The broken line exhibits the spacing–concentration relationship obtained on the assumption[3] that the end effect of the α-helical chains is negligible in dilution and that the α-helical chains are arranged in a hexagonal array; that is $d^2 = 133/c - 0.26$, where d is the spacing (nm) and c is the polymer concentration (wt%). Experimental data are in good agreement with the calculated line, indicating a homogeneous dispersion of a two-dimensional hexagonal arrangement of the α-helical chains in the solution, from a lower to a higher concentration. It is expected that the number and sharpness of the diffraction rings indicate the existence of the crystalline phase in the *m*-cresol solution above 41 wt%. It may be concluded from the continuous variation of the spacing of the inner diffraction ring that the *m*-cresol solution is transformed from a cholesteric liquid-crystal phase into a hexagonal semicrystalline phase, including solvent molecules. The α-helical molecules, which are distorted along the cholesteric twist axis, may be arranged parallel to each other to form small molecular blocks including solvent molecules, referred to as rod-like bodies in the discussion of the results on small-angle light scattering. This speculation may receive support from the sudden appearance of higher-order diffraction rings above 41 wt%, as shown in Figure 3(c).

In order to investigate the aggregated structure of the PMDG–*m*-cresol system above 41 wt%, small-angle light scattering (SALS) technique was used. Figure 4 shows small-angle light scattering patterns and a polarizing optical micrograph under crossed nicols for the solution of 49.7 wt% between two glass plates at 290 K. No retardation lines could be observed under our optical microscope, although the distance between the retardation lines was expected to be 1.5 μm, according to Robinson's empirical equation.[3] Four Debye rings were observed in the X-ray diffraction pattern of this solution of 49.7 wt%. Small optically anisotropic grains could be observed with a polarizing optical microscope and the small-angle light scattering patterns show the typical scattering diagrams from randomly oriented anisotropic rod-like particles. From the four fold $\pm 45°$ H_v pattern and the 0—90° V_v pattern, it appears that the main optical axes of the scattering elements orient parallel or perpendicular to the long axis of the rod-like body. Scattering elements of the α-helical chains may lie almost parallel to each other in the rod. Although the cholesteric liquid-crystal phase exhibited a similar $\pm 45°$ H_v scattering pattern, its optical activity distorted a four fold symmetry; that is, the scattering intensity distribution at the azimuthal angle of $+45°$ differs from that at $-45°$.[9,10] Thus, the H_v scattering pattern having the same intensity at $\pm 45°$ makes us expect an untwisted aggregation of the α-helical chains, such as the nematic or semi-

crystalline structure, in a solution above 41 wt%.

Measurement of circular dichroism (CD) is a useful technique for investigating the existence of a twisted structure such as the cholesteric liquid-crystalline structure. Tachibana[8] concluded from his circular dichroic study that the solid film of PMG cast from a 1,2-dichloroethane solution maintained a cholesteric structure; that is, the PMG film exhibited selective reflection of circularly polarized light in addition to cholesteric color. However, a solid film of PMDG cast from *m*-cresol showed no cholesteric color nor any apparent absorption of a circular dichroic curve due to the form circular dichroism ranging from 250 to 800 nm of wavelength. Therefore, it seems reasonable to conclude that the cholesteric-like twisted structure does not exist in the PMDG solid film cast from a *m*-cresol solution, in agreement with the results of the X-ray studies in the highly concentrated solution shown in Figure 3(c).

DSC measurement of PMDG solution in *m*-cresol was performed over a concentration range from 10 to 42 wt% and a temperature range from 200 to 400 K. DSC thermograms exhibited no distinct transition peaks other than the melting of the *m*-cresol solvent. In the case of a concentration above 20 wt%, the melting peak of solvent could no longer be observed because of the solvation of all solvent molecules. This indicates that these cholesteric liquid-crystal or paracrystalline phases including *m*-cresol solvent molecules are thermally stable.

Figure 5 is a schematic illustration for the solidifying process of a PMDG–*m*-cresol solution. In a cholesteric liquid crystal, α-helical chains lie in planes with a small helical twist relative to each other around a cholesteric axis perpendicular to the planes (Figure 5(a)). It has been reported that the helical twist angle between neighboring planes is proportional to the concentration to the power of 3/2, based on the X-ray diffraction study and optical microscopic observations.[3] Therefore, the twist angle increases with an increase in the concentration. This tendency results in that, at a critical concentration, the α-helical chains may become parallel to each other owing to advantage of the essentially parallel alignment. Paracrystalline regions do not necessarily have to be packed with the helical twist (Figure 5(b); cholesteric-like) with respect to the direction of the cholesteric axis existing formerly, since Figure 5(c) is more reasonalbe than Figure 5(b) according to the conclusion of the circular dichroic study as mentioned above.

Pyridine Solution (Group 2)

Figure 6 shows polarizing micrographs between crossed nicols for the PMDG–pyridine (Group 2 in Table I) system at the polymer concentration of 20.4 wt% which is above B-point. Figure 6(a) shows the solution gelatinized with high viscosity at 297 K.

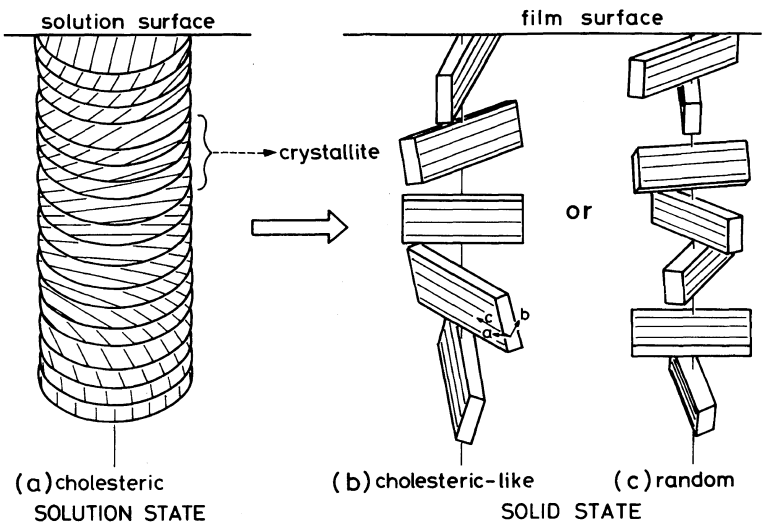

Figure 5. Schematic illustration for a possible solidifying process of a PMDG solution in *m*-cresol.

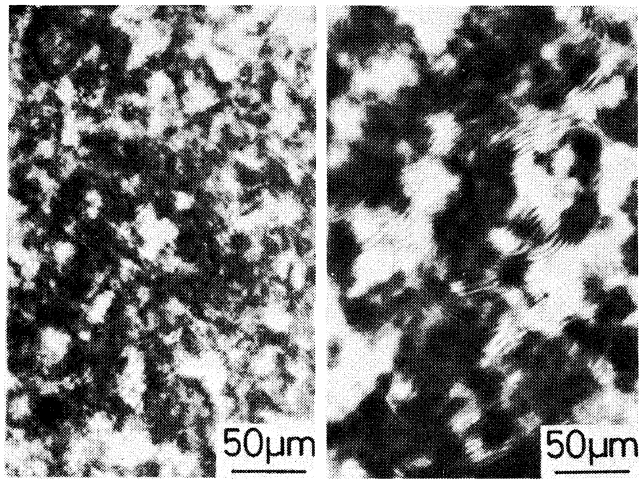

(a) (b)

Figure 6. Polarizing micrographs under crossed nicols for a 20.4 wt% PMDG solution in pyridine (a) at 297 K and (b) at 346 K.

Though this solution is anisotropic, no irridescent colors or equidistant retardation lines could be observed. On the other hand, Figure 6(b) is the same field of vision as Figure 6(a) at 346 K, for which retardation lines and irridescent colors could be observed. Retardation lines were reproduced at the same location in the reheating cycle. In the case of a lower concentration range from 14 to 18 wt%, spherulitic anisotropic liquid droplets could be observed, surrounded by an isotropic phase. The location of the liquid droplets had reproducibility during the heating and cooling cycles. Below 13 wt%, solutions remained isotropic at room temperature.

Figure 7 shows X-ray diffraction patterns and their schematic diagrams for PMDG solutions in pyridine at 298 K. As mentioned above, the solutions were gelatinized above a concentration of 5 wt% at 298 K. A single diffraction ring began to appear, together with a halo above 25 wt% as shown in Figure 7(a), but the sharpness of the ring was not as good as that of the *m*-cresol solution. When the concentration exceeded 41 wt%, another diffraction

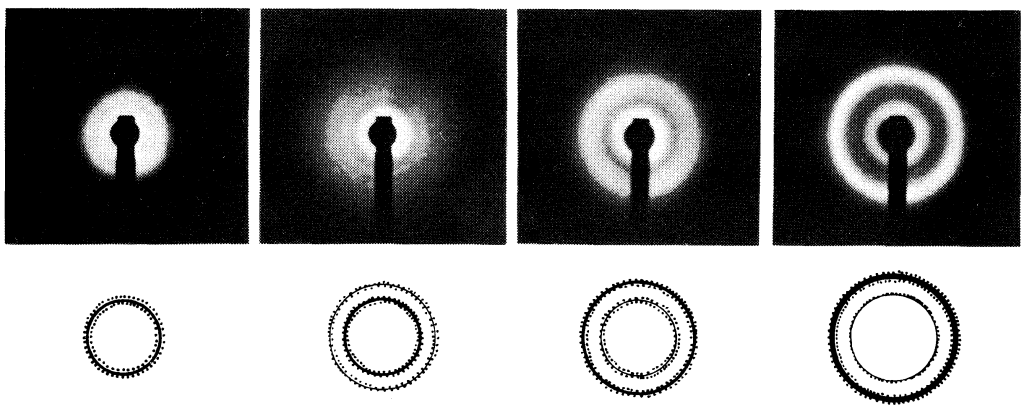

(a) 41.0 wt% (b) 50.6 wt% (c) 65.4 wt% (d) 76.6 wt%

Figure 7. X-ray diffraction patterns and their schematic illustrations of (a) 41.0 wt%, (b) 50.6 wt%, (c) 65.4 wt%, and (d) 76.6 wt% pyridine solutions at 298 K.

ring began to appear outside the first inner diffraction ring (at larger Bragg angle). The Bragg angles for these rings increased with increasing polymer concentration. The intensity of the inner diffraction was stronger in comparison with that of the outer ring in the lower concentration range (up to around 50 wt%), and the relative intensity of the outer ring increased with increasing concentration as shown in Figures 7(b), (c), and (d). The ratio of the reciprocals of the two spacings was 1 : 1.3—1.4. If these two diffraction rings are diffracted from a single phase, there is no explanation for the following three facts: (1) the only inner ring appeared at lower concentrations, (2) the intensities of these diffraction rings varied relatively in an opposite manner with an increase in the concentration, and (3) the only outer diffraction could be observed above 80 wt%. From the variation in relative intensity, the outer ring does not seem to be the higher-order diffraction of the inner ring but that it may arise from a different phase. It is expected that there are two phases in concentrated pyridine solutions (40—77 wt%): one may include a relatively large quantity of solvent and the another, a relatively small one. The mechanism for the coexistence of these phases is not known at present.

Figure 8 shows the X-ray diffraction diagram for a 45.6 wt% PMDG solution in pyridine at 335 K. Under this condition, the solution exhibited the retardation lines shown in Figure 6(b). Only one diffraction ring could be observed from the solution at 335 K.

Figure 9 represents a double logarithmic plot of the spacing of the diffraction ring against the polymer concentration obtained at 298 and 335 K for the PMDG–pyridine system. It is apparent that both spacings corresponding to the inner and outer rings could be observed at 298 K in the intermediate concentration region from 40 to 70 wt%. Since these spacings arise from the two different phases mentioned above, we tried to evaluate the fraction of these two phases after making correction for the base line, the Lorentz and the polarization factors for the X-ray diffraction intensities of the inner and outer rings. The overall concentration evaluated from the fractions and the concentrations based on the magnitudes of the observed X-ray spacings for the two phase were fairly comparable with the concentration of the specimen used. This fact seems to indicate that the two different phases with lower and higher concentrations may correspond to the liquid-crystalline phase and the paracrystalline phase in the hexagonal array of the α-helical chains, respectively. It is apparent that the liquid-crystalline phase may be nematic, from the reasons based on the circular dichroic and light-scattering experiments. The broken line representing the relationship of $d^2 = 141/c - 0.34$ was calculated on the assumption of a two-dimensional hexagonal array of the α-helical chains and no dilution along the molecular axes (negligible end effect of the α-helical axes).[3] Since the only one spacing at 335 K was observed with an intermediate magnitude between spacings for the inner and outer rings at 298 K, it may be possible that the two phases with higher and lower

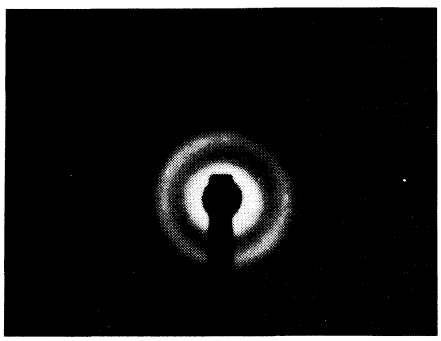

45.6 wt% PMDG solution in pyridine at 335 K

Figure 8. X-ray diffraction pattern for a 45.6 wt% PMDG solution in pyridine at 335 K.

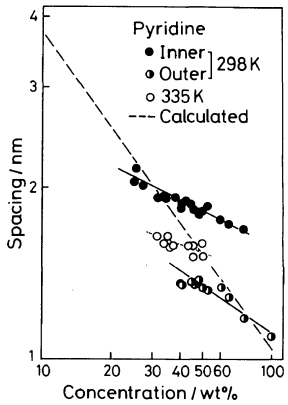

Figure 9. Polymer concentration dependence of the spacing for a PMDG solution in pyridine at 298 K (filled circle and half filled circle) and 335 K (open circle). The broken line is made from calculated values.[3]

concentrations at 298 K change into a fairly homogeneous phase at 335 K, accompanying the transformation from the gel to the cholesteric liquid-crystal phase.

Figure 10 shows the polarizing micrographs of (a) the 20 wt% solution in *m*-cresol at 300 K (Group 1 in Table I), and (b) the 20 wt% solution in pyridine at 335 K (Group 2 in Table I). In the case of the pyridine solution of (b), the cholesteric liquid-crystal domains were not well developed and their sizes were relatively small in comparison with the *m*-cresol solution of (a). Further, there were regions in which retardation lines could not be observed. These regions were different from the "plane texture" and hardly became homogeneous even on raising temperature. As will be mentioned later, free solvents, due to the development of syneresis, existed up to a concentration of 47 wt% at room temperature. Therefore, it is possible that a perfect mixing of the free solvent and the cholesteric phase could not have occurred by raising the temperature of the pyridine solutions. Since the apparent concentration of the cholesteric phase may be higher than that of the homogeneous solution, the X-ray spacing appeared to be smaller than the theoretical value (open circles in Figure 9).

The next point of interest is the thermal behavior of a pyridine solution accompanied by a phase transformation from the gel to the cholesteric liquid crystal. Figure 11 shows the DSC thermogram of a pyridine solution with a polymer concentration of 24 wt%. The DSC curve exhibited the endothermic peaks on heating (curve 1) and the exothermic peak on cooling (curve 2). When the solution was heated, three endothermic peaks were observed. The lowest temperature peak at about 235 K is responsible for melting of solvent. The intermediate and highest temperature peaks above 290 K may be related to the solution itself, in consideration of the optical microscopic observation to be mentioned later. A concentration dependence of the melting temperature of pyridine was not observed, suggesting the develop-

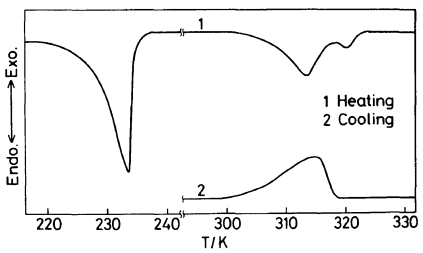

Figure 11. DSC thermogram for a 24 wt% PMDG solution in pyridine upon heating (curve 1) and cooling (curve 2).

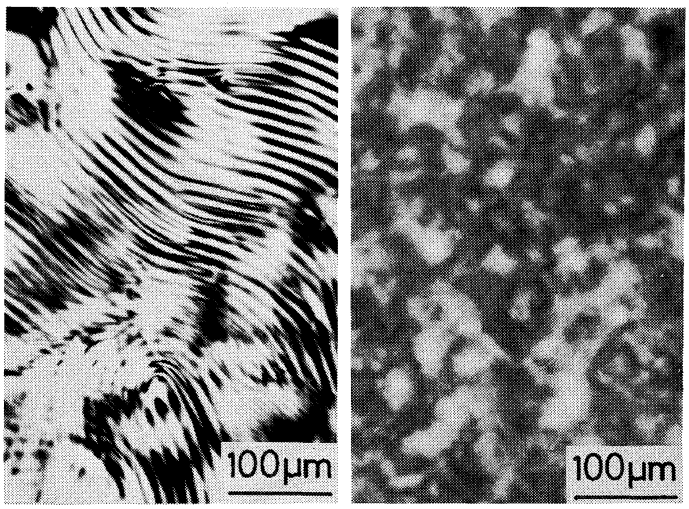

(a) *m*-Cresol (b) Pyridine

Figure 10. Polarizing optical micrographs under crossed nicols for 20 wt% solution in (a) *m*-cresol at 300 K and (b) pyridine at 335 K.

ment of a syneresis due to some shrinking of a gel network. The melting peak of the solvent disappeared above a concentration of 47 wt%, at which the outer X-ray diffraction ring began to appear (Figure 7). These results indicate that the disappearance of free solvents is accompanied by the growth of a more concentrated phase in the PMDG–pyridine system.

Figure 12 gives the concentration dependence of the intermediate peak temperatures on heating and cooling. The transition in a concentration range lower than the A-point of 13 wt% may be ascribed to the changes in an isotropic gel and solution as reported by Goebel,[11] since no X-ray diffraction peaks could be detected (Figure 9). The POM data were obtained from the polarizing optical microscopic observation under crossed nicols as follows. After the solution was heated until the cholesteric phase could be observed, it was allowed to slowly cool down to room temperature. The transition temperature from the cholesteric liquid-crystal phase to the gelatinized phase was then determined from the temperature at which the retardation lines and irridescent colors vanished. This means that the mesomorphic phase of cholesteric liquid crystal exists in the higher temperature region above the POM curve and the gelatinized phase is observed in the lower temperature region. Since the concentration dependence of the endothermic peak and exothermic peak temperatures respectively correspond fairly well to that obtained by microscopic observation, it is apparent that these thermal transitions are closely related to the phase transition between the cholesteric liquid crystal and the gel phases. From the fact that the solid films gave no similar transition peak, it is also evident that these transitions are related to the phase including the solvent. As mentioned above, the liquid crystal–gel transition of a solution exists in the evaporating process of the solvent (Figure 12). However, the solution state at the beginning of the evaporation of a solvent may still be important in influencing the aggregated state of α-helical chains in a solid film, since the mobility of α-helical chains decreases as the solvent evaporates and the aggregated structure in a solution can be maintained in the solid state.

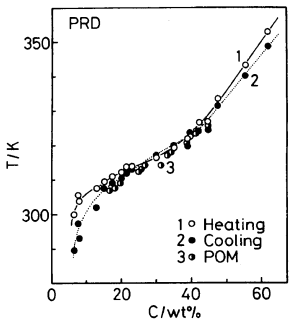

Figure 12. Concentration dependence of the transition temperature for a PMDG–pyridine system on heating (curve 1) and cooling (curve 2) based on DSC thermogram. POM data were obtained from polarizing microscopic observations.

Figure 13 shows the photographs of small-angle light scattering (SALS) and polarizing micrographs of a 27.9 wt% pyridine solution in the same field of vision at (a) 290 K and (b) 331 K, corresponding to temperatures below and above the transition peak temperature in Figure 12, respectively. Though both small-angle light scattering patterns for (a) the gel and (b) the cholesteric liquid crystal phases suggest the existence of rod-like aggregation based on the typical scattering diagram and the intensity distribution, the orientation of the scattering elements in the rod-like particle is different in each case. In the case of (a) the gel phase, the axis of the scattering elements may tilt $\pm 45°$ to the particle axis. On the other hand, in the case of (b) the cholesteric phase, the scattering elements may lie almost perpendicular or parallel to the particle axis. In the case of a PMDG solution and a solid film, the scattering elements may consist of α-helical chains. Although there may be differences in the manner of packing, both have a tendency for parallel arrangement in a concentrated solution due to the rigid character of the α-helical chains.

Figure 14 is a plot of the reciprocal of the cholesteric pitch *vs.* temperature for a 20.4 wt% pyridine solution. The broken line represents the transition temperature between the cholesteric liquid crystal and the gel phases shown in Figure 12. The reciprocal of the pitch, $1/P$, increased with decreasing temperature, showing the tendency of P to approach zero with a decrease in temperature. This trend indicates the existence of a parallel aggregation of the α-helical chains in the gel state. As mentioned above, the two different phases in the gel state may be of the paracrystalline and the liquid-crystalline

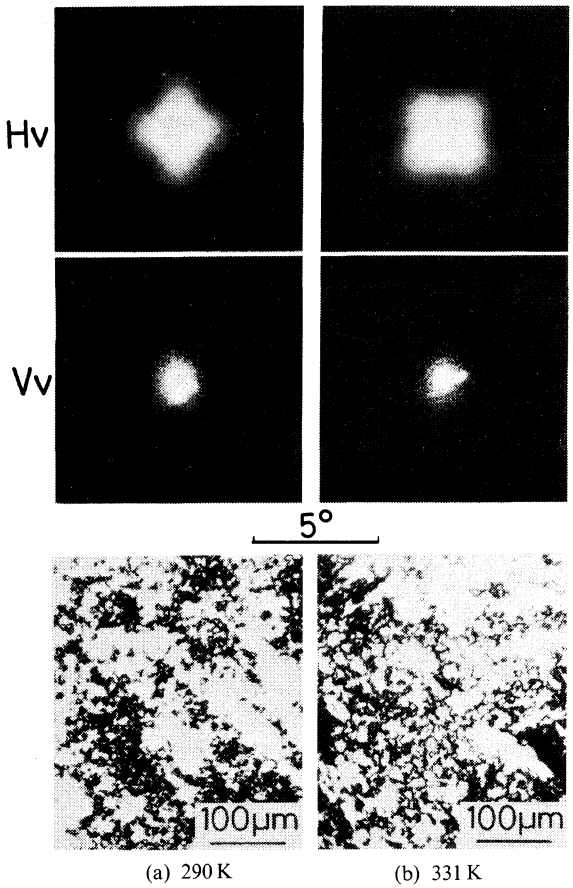

(a) 290 K (b) 331 K

Figure 13. Small-angle light scattering (SALS) patterns and polarizing micrographs under crossed nicols for a 27.9 wt% PMDG solution in pyridine at (a) 290 K and (b) 331 K.

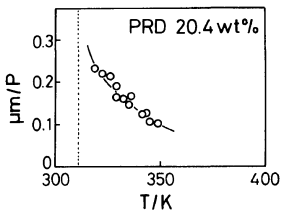

Figure 14. Temperature dependence of reciprocal of the pitch, $1/P$ for a 20.4 wt% PMDG solution in pyridine. The broken line corresponds to the transition temperature in Figure 11.

phases. Neither of these phases may have spiral structures as a result of the $1/P$–T relationship. This indicates that the latter liquid-crystalline phase corresponds to the nematic phase.

The bright portion in the polarizing optical micrograph under crossed nicols as shown in Figure 13(a) may represent anisotropic rod-like bodies in which the axes of the α-helical chains tilt $\pm 45°$ to the axes of the rod-like bodies. Therefore, the thermal transition behavior shown in Figures 11 and 12 may be responsible for transforming the anisotropic portion in the gel network into the cholesteric liquid-crystal structure.

Figure 15 represents the electron micrographs of PMDG cast from 0.05 wt% 1,2-dichloroethane (Group 1) and pyridine (Group 2) solutions. In the case of pyridine in Figure 15(b), fibrils 20—30 nm wide could be observed, indicating that some interaction by means of fibrillar branches among fibrous bundles occurred in the solidifying process. Such a tendency to form a network composed of fibrous bundles could generally be observed for PMDG cast from solutions of Group 2 solvents in Table I. However, in the case of PMDG cast from solutions of Group 1 solvents (Figure 15(a)), this tendency to form a network of fibrils could not be observed, though bundle-like aggregates were noticed.

1,2-Dichloroethane Solution (Group 1)

So far, the classification of solvents into Groups 1 or 2 was performed on the basis of the solution state (cholesteric liquid crystal or gel) at room temperature and the orientation of the α-helical chains in solid films cast from these solutions.[1] Solvents belonging to Group 2 at room temperature were classified into Group 1 at higher temperatures. Therefore, as a general trend, solvents of Group 1 have the character of Group 2 at low temperatures, *vice versa*. 1,2-Dichloroethane (DCE) is a good representative of a Group 1 solvent for making sure whether this expectation is correct or not, because only the dichloroethane solution of PMG exhibited a transition peak, except for the melting peak of the solvent, on a DSC curve.

Figure 16 shows the concentration dependence of the transition peak temperature upon heating and cooling. Since the transition could not be observed at a concentration lower than the A-point, it is apparent that the transition peak is in close relation to the cholesteric liquid crystalline state. The transition peak was endothermic and exothermic on heating and cooling, respectively. The profile of the DSC

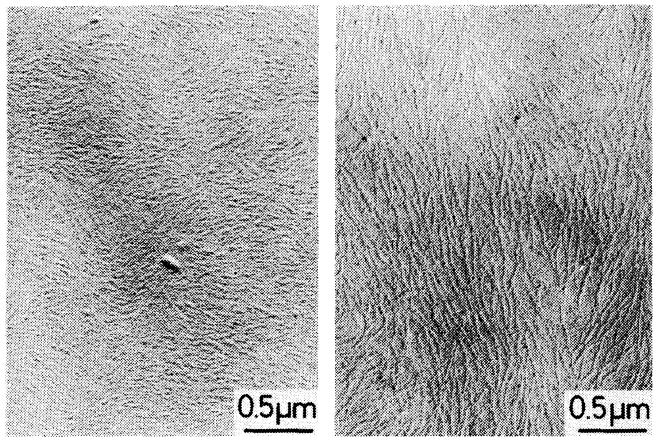

(a) DCE (b) PRD

Figure 15. Electron micrographs for PMDG cast from (a) 0.05 wt% dichloroethane and (b) 0.05 wt% pyridine solutions.

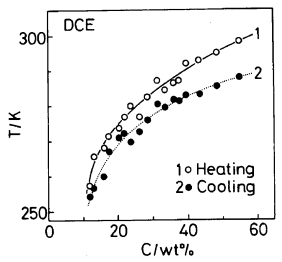

Figure 16. Concentration dependence of transition peak temperatures on heating (curve 1) and cooling (curve 2) for a PMG–dichloroethane system.

curve was similar to that of a pyridine (Group 2) solution as shown in Figure 11, except that the peak was single on heating and relatively sharp on cooling. The absorbed heat on heating was constant at about 0.1 kJ mol^{-1}-residues in the concentration range studied here. The magnitude was comparable to that generally observed for the transition from smectic-C to smectic-A in a thermotropic liquid crystal with low molecular weight.[12] On the other hand, the melting peak of solvent could be observed as far as 55 wt% at which the number of solvent molecules per one residue of PMLG was 1.2. This may suggest that polymer–solvent interaction may be fairly weak. In order to investigate the phase change above and below the transition temperature, we carried out polarizing optical microscopic observations under crossed nicols.

Figures 17(a) and (b) show polarizing micrographs (crossed nicols) of the PMLG–dichloroethane system having a concentration of 22.9 wt% at 265 and 293 K in the same field of vision. These temperatures correspond to the temperature range below and above the concentration–transition temperature curve, respectively. Retardation lines characteristic of the cholesteric liquid crystal could be observed in (b), while only a trace of these lines could be seen in (a). Also, in the temperature range below the transition, the solution became turbid and paste-like.

Figure 18 is a plot of the reciprocal of the cholesteric pitch against temperature. The broken line represents the transition temperature on cooling (curve 2 in Figure 16) at each concentration. $1/P$ rapidly increased with a decrease in temperature, suggesting that broken lines correspond to the temperatures at which $1/P$ becomes infinity (P approaches zero), indicating the transition to the nematic structure. In other words, the cholesteric pitch gradually decreases with decrease of temperature and the twist angle between neighboring cholesteric planes increases. This tendency seems to induce the structural transformation from cholesteric to nematic phase. However, the high viscosity of the solution did not allow time to observe a nematic structure. In conclusion, a 1,2-dichloroethane solution does have a transition temperature other than the melting of the solvent. This transition may be related to the phase change of cholesteric–nematic or cholesteric–gel, as in the case of the Group 2

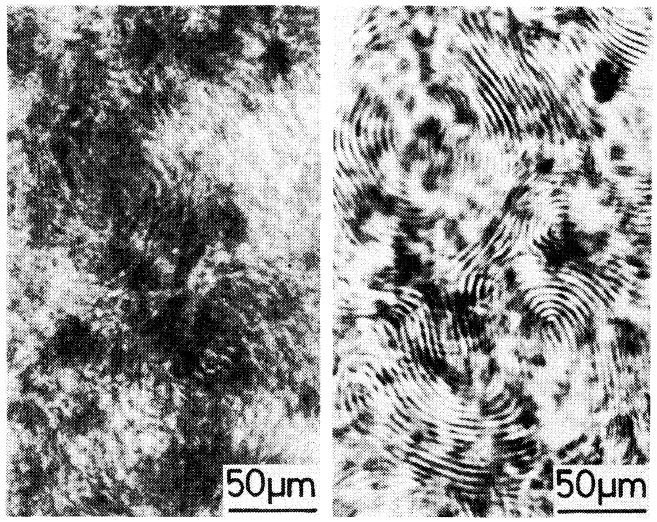

Figure 17. Polarizing micrographs for a 22.9 wt% PMLG solution in dichloroethane under crossed nicols at (a) 265 K and (b) 293 K; both photographs are in the same field of vision.

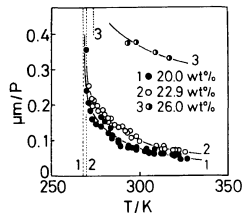

Figure 18. Temperature dependence of the reciprocal of the pitch, $1/P$ for the PMLG–pyridine system with polymer concentrations of 20.0 wt% (curve 1), 22.9 wt% (curve 2) and 26.0 wt% (curve 3). The broken lines correspond to the transition temperatures in Figure 15.

solutions. Recently, liquid-crystal induced circular dichroism (LCICD) on cholesteric liquid crystal was reported.[13] A mixture of achiral dye molecules and cholesteric liquid crystals exhibits circular dichroic absorption at the absorption band of the dye induced by the cholesteric twisted structure. The application of the LCICD to our system will confirm the existence of the cholesteric–nematic transition.

CONCLUTIONS

The aggregated states of the α-helical chains of PMG in solution were investigated by X-ray diffractometry, DSC, and small-angle light scattering measurements, and optical microscopic observation. In the *m*-cresol system, molecular chains are homogeneously dispersed and packed in a two dimensional hexagonal array in cholesteric liquid-crystalline and paracrystalline phases including solvent molecules, in order of increasing concentration. The planar orientation is formed in the solid film when the film is cast passing through a cholesteric liquid crystal. In the pyridine system, the solution was gelatinized and molecular chains were heterogeneously dispersed in the gel at lower temperatures. On the other hand, the gel transforms to a fluidizable solution exhibiting the characteristics of the cholesteric liquid crystal at higher temperatures, but the solution is not perfectly homogeneous. The temperature dependence of the cholesteric pitch indicates a mixture of a nematic-like structure in the gel phase. The mechanism for the aggregated structure proposed here is still in its initial stage. We hope that this study will serve as the basis for further clarification of the aggregated states of PMG in a concentrated solution.

Acknowledgement. The authors offer their grateful acknowledgement to Ajinomoto Co., Ltd. for providing poly (γ-methyl glutamate) samples.

REFERENCES

1. K. Ito, T. Kajiyama, and M. Takayanagi, *Polym. J.*, **9**, 355 (1977).
2. C. J. Heffelfinger and R. L. Burton, *J. Polym. Sci.*, **47**, 289 (1960).
3. C. Robinson, J. C. Ward, and R. B. Beevers, *Discuss. Faraday Soc.*, **25**, 29 (1958).
4. V. Luzzati, M. Cesari, F. Masson, and J. M. Vincent, *J. Mol. Biol.*, **3**, 566 (1961).
5. D. A. D. Parry and A. Elliott, *Nature*, **206**, 616 (1965).
6. D. A. D. Parry and A. Elliott, *J. Mol. Biol.*, **25**, 1 (1967).
7. E. T. Samulski and A. V. Tobolsky, *Mol. Cryst. Liq. Cryst.*, **7**, 433 (1969).
8. T. Tachibana and E. Oda, *Bull. Chem. Soc. Jpn.*, **46**, 2583 (1973).
9. C. Picot and R. S. Stein, *J. Polym. Sci., A-2*, **8**, 1491 (1970).
10. S. Ebis, T. Hashimoto and H. Kawai, *Polym. Prepr., Jpn.*, **28**, 320 (1979).
11. K. D. Goebel and W. G. Miller, Macromolecules, **3**, 64 (1970).
12. A. Saupe, "Liquid Crystals & Plastic Crystals," G. W. Gray and P. A. Winsor Ed., Halsted Press, New York, N.Y., p 22, (1974).
13. F. D. Saeva and G. R. Olin, *J. Am. Chem. Soc.*, **95**, 7882 (1973).